Resonance, edited by W. Low (Academic, New York, 1963), Vol. II, p. 447.
[16]R. G. Shulman, B. J. Wyluda, and P. W. Anderson, Phys. Rev. 107, 953 (1951).
[17]R. Calvo, R. A. Isaacson, and Z. Sroubek, Phys. Rev. 177, 484 (1969).
[18]N. S. Shiren, in *Proceedings of the Twelfth Colloque Ampère, Eindhoven*, 1962, edited by J. Smidt (Interscience, New York, 1963).
[19]The form of the master rate equations is well known; see, for example, Andrew and Trunstrall, Proc. Phys. Soc. (London) 78, 1 (1961).
[20]B. V. Haxby, Ph. D. thesis (University of Minnesota, 1957) (unpublished).
[21]R. L. Hansler and W. G. Sogelken, J. Phys. Chem. Solids 13, 124 (1960).

PHYSICAL REVIEW B VOLUME 4, NUMBER 9 1 NOVEMBER 1971

Ranges of Recoil Atoms from the (n,γ) Process

William R. Pierson, Joseph T. Kummer, and Wanda Brachaczek
Scientific Research Staff, Ford Motor Company, Dearborn, Michigan 48121
(Received 24 February 1970; revised manuscript received 21 January 1971)

Ranges of ^{198}Au (estimated average energy 50 eV) recoiling from neutron capture in gold film surfaces have been estimated in deuterium, helium, neon, argon, and xenon by measuring the yield on a collector as a function of gas pressure. These ranges are 0.3, 0.54, 1.1, 0.8, and 1.2 μg/cm^2, respectively. From the shape of the curve of recoil yield vs pressure in helium, the range is inferred to be largely independent of energy; this contrasts with the strong dependence known to hold at higher energies. A simple model such as that used for neutron thermalization reproduces the magnitudes and trends of the ranges reasonably well.

INTRODUCTION

The work to be described in this paper deals with ranges of atoms in the 100-eV region of kinetic energy, and with the angular distribution of such atoms when ejected from surfaces. Range measurements in this energy region have not heretofore been attempted, to our knowledge.

An extrapolation of data obtained at higher energies[1–12] suggests that, at 100 eV and less, ranges should be about one interatomic distance. The few indications that actually exist in this energy region are all from (n,γ) recoil studies[13–19] as far as we know, and for the most part these studies indicate that the ranges are of the order of 1 to 10 interatomic distances.

Our method of measurement depends on the fact that an atom recoiling from emission of a γ ray has a kinetic energy

$$E = E_\gamma^2/2Mc^2. \quad (1)$$

(Here, E_γ is the energy of the γ ray, M is the mass of the recoiling atom, and c is the velocity of light.) In the case of neutron-capture γ rays, the recoil kinetic energy is of the order of 100 eV. Recoiling atoms which are ejected from a solid surface are allowed to cross a gas-filled gap to a collector. The number of recoil atoms reaching the collector is measured as a function of gas pressure. With the gap evacuated, a certain number of recoil atoms will reach the collector. As the pressure goes up, more and more atoms are slowed to thermal energy in the gas and diffuse to either the collector or the surface of origin. At sufficiently high pressure, essentially all of the atoms will be thermalized within a short distance and very few will reach the collector. By allowing for diffusion, a projected range can be deduced from such data. Then, with some knowledge of the angular distribution of emitted recoils, the range can be estimated.

The range information obtained in this way is quite crude. First of all, the recoil motion and diffusion are not strictly separable. Second, the recoiling atoms are widely distributed in velocity, both in magnitude and direction. Even so, some interesting trends can be seen despite the limitations.

EXPERIMENTAL METHOD

The atoms used in this study are ^{198}Au ejected from gold surfaces by the process ^{197}Au$(n,\gamma)^{198}$Au; ^{198}Au is a β and γ emitter of 2.7-day half-life, and so the number of recoil atoms reaching the collector can be ascertained by the usual means of counting radioactivity, long after the recoil processes have occurred.

The (n,γ) process on ^{197}Au leads to a level in ^{198}Au at 6.5 MeV.[20] The deexcitation from this level is prompt ($\ll 10^{-6}$ sec) and proceeds to the ground state by a complex decay scheme involving a number of alternate pathways (γ-ray cascades). The path consisting of direct transition to the ground state, with emission of a single γ ray of energy 6.5 MeV, is followed only about 2% of the time; the recoil energy [Eq. (1)] in this case would be 115 eV. The rest of the time the recoil energy

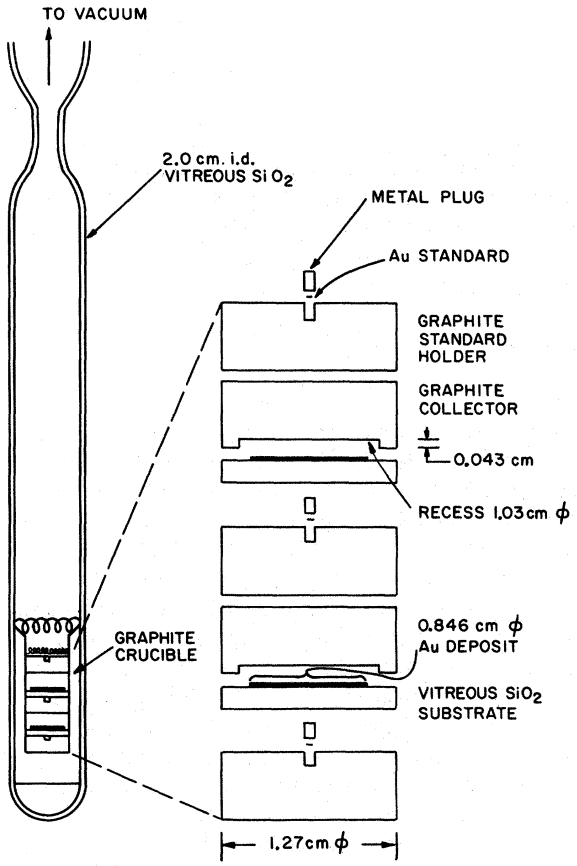

FIG. 1. Apparatus used for range measurements. On the left is shown the silica tube containing the assembled contents. On the right is an exploded view, on a larger scale, of the contents of the graphite crucible.

will be less, determined by the energies of the γ rays in a particular cascade and by the (essentially random) directions in which the γ rays happen to be emitted with respect to each other. There will tend to be one high-energy γ ray in each cascade, and, because the recoil energy varies as the square of the γ-ray energy, the recoil motion will be governed by that γ ray. Random-walk calculations on some representative situations suggest that the probability distribution of recoil momenta imparted in neutron-capture γ-ray cascades is approximately symmetric about a mean of 60–80% of the maximum observed (see Figs. 3 and 7 of Ref. 21). The average recoil energy obtained from such a momentum distribution is approximately half the maximum. In the present case, this average is about 50 eV. There are, however, recoil atoms with energies up to 115 eV and as low as perhaps 5 eV.

Range Measurements

The apparatus for the range experiments is depicted in Fig. 1. The source is a gold film some 2000–5000 Å thick and 0.847 cm in diameter, sputtered in an argon atmosphere onto a vitreous-silica disk of diameter 1.27 cm. Across a gap of 0.043 ± 0.002 cm there is a graphite collector that subtends a solid angle of 2π sr from all points in the target surface. Above and below this sandwich there are small pieces of gold wire, each of weight approximately 100 μg (known to ±1%). Knowing the activity induced per unit mass in these gold wires, one calculates the amount of activity expected to be induced in one atomic layer of the gold film. Measurement of the activity found on the collector then permits one to determine what fraction of the ^{198}Au atoms produced per layer of gold reaches the collector.

Normally, in each run there are two source-plus-collector sandwiches and three standards, as represented in Fig. 1, held in a graphite crucible. All graphite used is high-density reactor-grade material, fired in an atmosphere of argon just before use.

After sputtering, the components are assembled and the loaded crucible is put into a vitreous-silica tube and evacuated with a liquid-nitrogen-cooled molecular-sieve pump and further evacuated with a sputter-ion pump. The final pressure in the space between the film and collector is estimated to be $< 5 \times 10^{-5}$ mm Hg.

After pumpdown, the gas in which the range is to be determined—He, D_2, Ne, Ar, or Xe—is admitted to a pressure of 2.5–760 mm Hg. The silica tube is then sealed off and irradiated with neutrons. From the known capture cross section of gold and the irradiation conditions it can be estimated that only about one ^{197}Au nucleus in 10^7 will capture a neutron during such an irradiation; accordingly, the alteration of the gold surface by departing recoils is inconsequential.

The role of fast neutrons is probably negligible, since the cadmium ratio (loosely speaking, the ratio of neutron abundances below and above 1 eV) is about 8 or 9 in the pile locations employed. Experimentally, varying the cadmium ratio (by changing irradiation locations in the pile) had no discernible effect on the results—an indication that the role of fast neutrons is not significant. It is necessary that this be so if the experiment is to be successful, because a relatively large recoil energy (tens of keV) would be imparted by the impact of a fast neutron.

There could be a significant perturbation of the experiment if electric fields happen to be present, since some (perhaps one-half[14]) of the recoiling ^{198}Au species are ions. We have done experiments with the source electrically connected and unconnected to the collector and have observed no significant difference in the results; these experiments were with the gap evacuated, however, and the conconclusion might not apply at higher pressure.

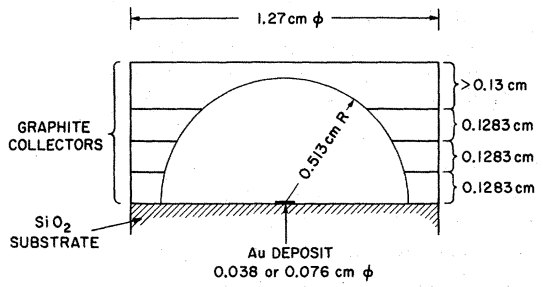

FIG. 2. Sample used for the angular-distribution measurements. This sample is loaded into the graphite crucible with standards above and below, as in the range measurements (Fig. 1).

Several hours after irradiation, the pieces are counted for ^{198}Au content by measuring the intensity of the 411-keV γ ray that accompanies the decay of ^{198}Au. This is done with a 7.6-cm-diam × 7.6-cm-thick NaI (Tl) crystal connected to a 400-channel pulse-height analyzer. The γ-ray spectrum is analyzed by stripping out the background together with any energetic γ ray. The uncertainty in the measurement is a few percent.

From the counts on standards and collectors and from the area of the gold film and the lattice parameters for gold, we determine what fraction of the ^{198}Au produced in the top layer of the gold film is found on the collector. It is necessary to make a correction for the gold in the collector that did not arrive there by recoil (that is, gold already present as an impurity in the graphite or gold that might have been transferred by accidental contact of the collector with the film, and so forth). This correction is evaluated by reirradiating the collectors together with some standards after the originally induced ^{198}Au has decayed. This bulk-gold correction in a properly done experiment is approximately $\frac{1}{2}$% of the original activity.

Several experiments of the kind just described were performed with each gas, one experiment for each of a number of different pressures to obtain a curve of activity collected vs pressure.

Angular-Distribution Measurements

The assembly for the angular-distribution experiments is shown in Fig. 2. The diameter of the target (gold film) is nominally 0.038 or 0.076 cm, and is measured to within ±2% with a toolmaker's microscope. To make the four-piece collector, four 1.27-cm-diam graphite disks—three of them 0.1283 ± 0.0025 cm thick and the fourth one thicker—are clamped together. A hemisphere of radius 0.513 ±0.0025 cm (i.e., 4×0.1283) is hollowed out of the stack in such a way that the hemispherical surface of radius R is divided into four parallel slices by equidistant planes spaced $\frac{1}{4}R$ apart. The four curved graphite surfaces comprising the hemisphere thus have equal areas. Hence if, for example, the emission of recoil atoms is isotropic, equal activities should be found on the four segments.

The rest of the procedure resembles that for the range measurements, except that no gases are admitted after pumpdown. The assembly is pumped down to the 10^{-6} mm Hg range as read at the pump, or an estimated 5×10^{-6} mm or better in the space between the film and collectors.

RESULTS

Range Measurements

The results for the recoil activity reaching the collector as a function of the amount of material penetrated[22] are shown in Fig. 3 and in the middle column of Table I. The ordinate in Fig. 3 is the activity collected relative to that which would have been collected if every surface gold atom undergoing neutron capture had recoiled into the collector. In calculating this we take the packing of gold atoms in the surface layer to be that calculated for the (111) face of gold, 1.4×10^{15} atoms per cm^2. [X-ray scans of several of our films have shown that these films are consistently, and essentially wholly, oriented (111).] Some other basis would merely change the scale and is of no great importance for the present purpose. The value at 0 μg/cm^2 is actually from a great number of determinations and of course is the same for each plot. (This value is considerably higher than that obtained by other investigators,[15,16] who were using foils; we have observed, with evaporated films and with sputtered films subjected to annealing, that recoil yields are somewhat dependent on the nature of the surface.)

We find the following:

(i) The projected ranges do *not* exhibit any pronounced trend with atomic or molecular weight of the gas penetrated (judging by the amount of ma-

TABLE I. Estimated ranges of ^{198}Au recoiling from ^{197}Au$(n,\gamma)^{198}$Au.

Gas penetrated	Range (μg/cm^2) Raw[a]	Corrected[b]
D_2	0.5	0.3
He	0.72	0.54
Ne	1.1	1.1
Ar	0.8	0.8
Xe	1.2	1.2

[a]This is the amount of material needed to halve the recoil activity reaching the catcher (see arrows in Fig. 3).

[b]These values are obtained by applying corrections for angular distribution, diffusion, etc., as described in the Analysis section of the paper.

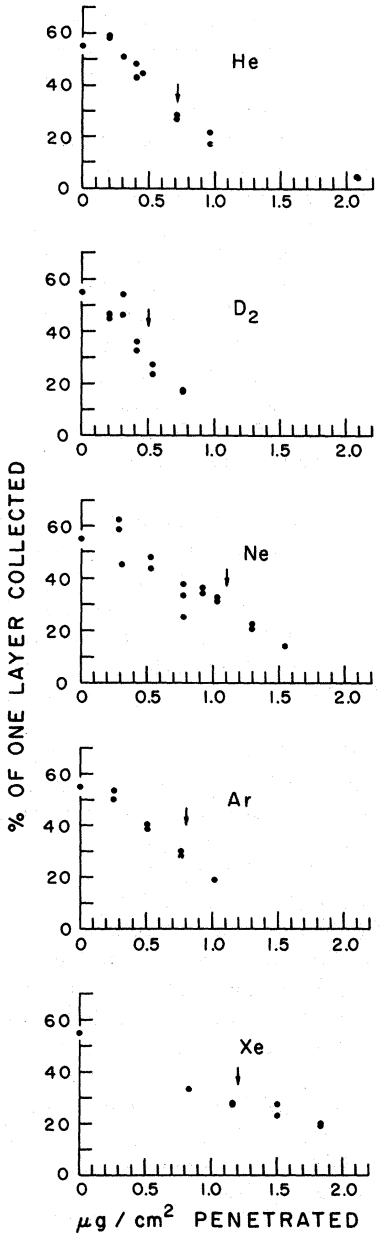

FIG. 3. Recoil ^{198}Au activity collected vs mass of material penetrated, for various stopping materials as indicated. Activity collected is expressed as a percentage of that which would have been collected if every ^{198}Au produced in the surface were to recoil into the collector and if the surface were entirely oriented (111). The point where the yield has dropped to one-half its value in vacuum is indicated on each plot. For explanation of abscissa see Ref. 22.

terial needed to cut the collected activity in half—arrows in Fig. 3 or the middle column of Table I).

(ii) There is a difference between the range in He and the range in a gas of diatomic molecules of the same mass (deuterium).

(iii) The shape of the plot in the case of He is what would be expected for a *monoenergetic collimated* beam of gold atoms or ions. If the emission of recoil atoms from the gold surface were isotropic, such a plot could not be obtained.[23] Further, even if the emission were unidirectional, with a large spread in energy, such a plot could still not be obtained *unless* the range was somewhat independent of energy. We might say that the profile in He is suggestive of a monorange collimated beam of gold.

Angular-Distribution Measurements

The results of the angular-distribution measurements are shown in Fig. 4, along with the results that might have been expected if the emission were isotropic into the full 2π sr in the forward direction or, alternatively, distributed about the surface normal in the cosine distribution characteristic of particles evaporating at thermal energies.[24–26] The experimentally observed distribution seems to favor the direction perpendicular to the emitting surface; with annealed films (not shown) this forward peaking is quite pronounced, the distribution departing strongly from the "cosine law."

There seems to be excess emission sideways (collector 1 of Fig. 4). Possibly this "side lobe" is spurious; if, in making the film, gold deposited on the substrate were to extend sufficiently beyond the boundaries of the intended film area, it might later be rubbed off onto the bottom collector. An alternative hypothesis is that the sticking probability in a gold impact onto graphite is less than unity and that some of the recoils find their way to collector 1 by scattering. We rule out the latter hypothesis—scattering—because of evidence that the

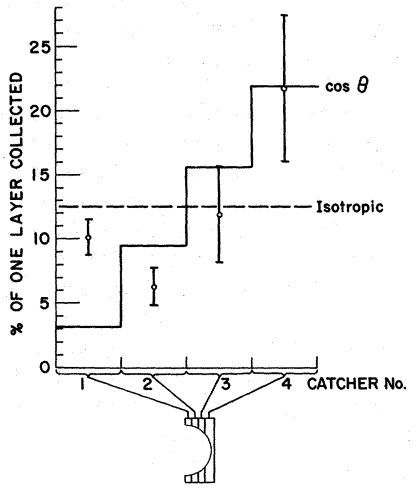

FIG. 4. Angular distribution of ^{198}Au recoiling out of the solid surface. Shown for comparison is the distribution that would have been obtained if the emission were isotropic into 2π sr and the distribution that would have been obtained if the emission followed a cosine law.

sticking probability of these recoils in the graphite is close to 1.0. The nature of this evidence is a series of experiments in which the geometry of the collector surface was arranged in such a way that it would catch all recoils, whether there was scattering or not (conceptually, the arrangement is one in which the collecting surface is a cavity, with a tiny opening where the gold film sits). The recoil fraction from these experiments was found to be the same as the recoil fraction from experiments using the usual collector geometry like that shown in Fig. 1, demonstrating that scattering is not important.

On the other hand, the side lobe in Fig. 4 cannot be explained by gold on the substrate outside the intended boundary, because that would yield an increase in the total recoil activity, which was not found.

ANALYSIS

Corrections to Raw Range Data

The range results given in the previous section should be corrected for such factors as diffusion and angular distribution in order to arrive at a better estimate of the range. In this section we will attempt to correct for these factors. The ranges thus obtained are given in the last column of Table I.

Assume, as a reasonable approximation to Fig. 4, that the angular distribution of emitted recoil atoms (i.e., the relative probabilities of emission in various directions) follows Knudsen's[25] cosine law, i.e., that, as measured with reference to an axis perpendicular to the surface, the probability of emission at angle θ into unit solid angle is proportional to $\cos\theta$. As the recoiling atoms approach thermal equilibrium with the gas that comprises the stopping material, they find their way either to the collector or to the source or its substrate, where presumably they stick. During the travel, diffusion is constantly operative and becomes the predominant mode of motion in the later stages. In principle, the end of the range is reached when the recoil component of the motion has been reduced to zero and random thermal motion has been established. Strictly speaking, this requires an infinite number of collisions. In practice, a limit to the range of a given atom is reached when the recoil momentum perpendicular to the collector plane falls to zero or passes through zero, which occurs when the scattering angle reaches 90°; subsequent steps have components toward source and collector with equal likelihood (see the Appendix). Concurrently, the recoil motion will be spread out and eventually truncated by diffusion to the absorbing surfaces.

When the recoil atom reaches the effective end of its range within the gas, the subsequent path of the atom can be treated as a random walk with absorbing barriers and variable-length steps ("gambler's ruin" problem),[27] provided that the longest step (distance between collisions) is short compared to the distance between boundaries (the gap). Consider the experiments in helium, where scattering angles and energy transfers per collision are smallest and therefore straggling should be at a minimum. Assume that the particles have a single range r and an angular distribution proportional to $\cos\theta$. Let x denote the projection of the range onto an axis normal to the emitting surface. Then the density distribution of x is proportional to x for $x \leq r$, and zero for $x > r$. If now the diffusion problem is weighted by this range-projection distribution, the profile of recoil fraction vs amount of gas penetrated comes out as shown in the line of Fig. 5. We have ignored the fact that the *effective* angular distribution must be different from the distribution in vacuum; that is, the distribution defined by the initial recoil directions will not be maintained to the range end points if the latter are defined as the point at which the recoil has been deflected by 90°.

We see that the calculated curve passes through $A_d/A_0 = 0.5$ at $d/r = 1.33$. Our experimental helium data give $A_d/A_0 = 0.5$ at $d = 0.72$ $\mu g/cm^2$ (Fig. 3), which thus implies $r = 0.54$ $\mu g/cm^2$ in helium. If the helium experimental points (Fig. 3) are scaled by this r, they appear on Fig. 5 as shown. (Included in Fig. 5 are a pair of points at $d/r = 14.3$ omitted from Fig. 3.) The fit seems to deteriorate at large d but, even apart from any attempt to allow for diffusion or the angular distribution, the effective range in He is undoubtedly close to the number cited.

The range in deuterium, estimated in the same manner as above, is 30% less than the range in helium. Possibly this reflects simply a difference in collision cross section.

For Ne, Ar, and Xe, progressively fewer collisions occur before the end of the range is reached, and the maximum deflection per collision (see the Appendix) increases. Hence straggling should be enormous and one should not think of the range end points as having a $\cos\theta$ probability distribution about the surface normal, but rather something more nearly isotropic. (The S shape characteristic of He in Fig. 3 seems less obvious in the heavier gases, as if to bear this out.) An isotropic distribution of range end points would project onto the surface normal as a rectangle with, as before, a cutoff at $x = r$. With subsequent diffusion, the range r in these cases would be equal to the value of d at which $A_d/A_0 = 0.5$ (the places marked with arrows in Fig. 3). This r is only $\frac{4}{3}$ that calculated on the assumption (employed in the He and D_2 an-

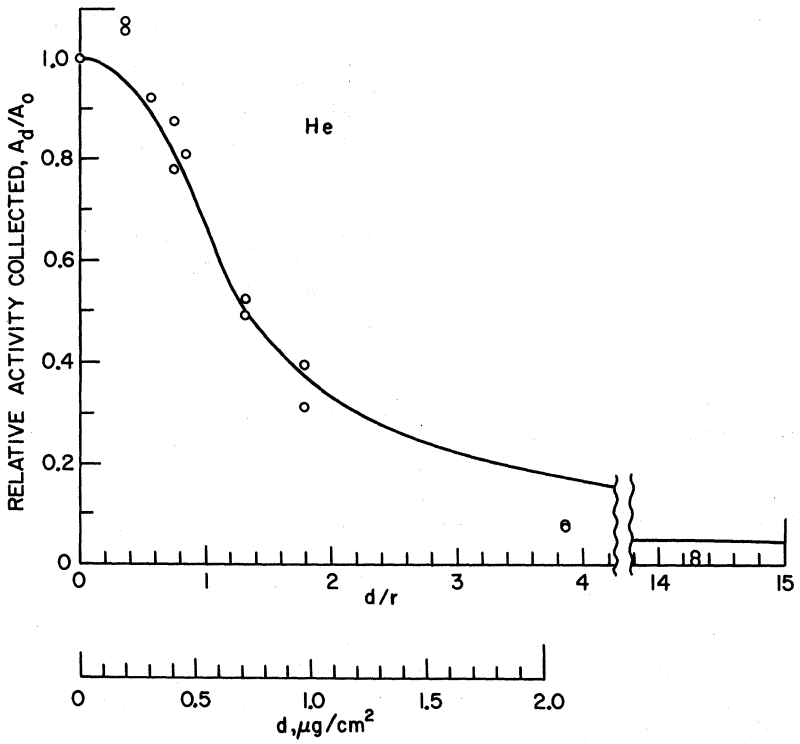

FIG. 5. Estimation of range by comparison of predicted and experimental collected recoil activity as a function of gas pressure (in a light gas). The ordinate is the activity collected, normalized to the activity collected in vacuum (gap $d=0$). For the predicted curve we assume the recoil atoms to be emitted in a $\cos\theta$ angular distribution, all with equal range r, with ordinary diffusion commencing after the particle reaches the end of its range. The upper abscissa is the ratio of the gap d to the range r. The experimental points are the helium data (from Fig. 3) with the lower abscissa scaled to correspond to a range $r=0.54$ $\mu g/cm^2$.

alyses) that there is no straggling, which suggests that the perturbation of the initial angular distribution will not affect the results radically. Curves calculated on the basis of isotropic distribution reproduce the experimental points for Ne, Ar, and Xe reasonably well.

The ranges, estimated as outlined, are summarized in the last column of Table I. The trend of corrected range with mass, like the trend of the raw range, is slight.

Comparison of Experimental and Expected Ranges

We suggest the following rationalization for the magnitude of the range in helium (Table I):

In the energy region with which we are dealing, energy loss is accomplished primarily by elastic collisions. In a series of elastic collisions between a target of mass m_2 at rest and a projectile of mass m_1 and kinetic energy E_0, the average number of elastic collisions necessary to reduce the kinetic energy to some value E is

$$\bar{n}=\left(\ln\frac{E_0}{E}\right)\Big/\left(\frac{(m_1-m_2)^2}{2m_1m_2}\ln\frac{m_1-m_2}{m_1+m_2}+1\right) \qquad (2)$$

if the scattering is isotropic in the center-of-mass system (i.e., if the potential is hard sphere) and if the cross section is independent of the energy. (This can be derived in a manner similar to the derivations given in Refs. 28 and 29 for the special case of neutron thermalization.)

With $E_0=50$ eV, $E=0.038$ eV (thermal energy), and the masses m_1 and m_2 of Au and He, 170 collisions are necessary, on the average, to slow the gold recoil atom to thermal energy in helium. The mean free path λ of Au in He is about 0.0033 $\mu g/cm^2$ (judging from the He atomic radius from viscosity measurements,[30] combined with the atomic radius of Au). Thus, the estimated mean *path length* (*not* displacement, although only slightly greater than the latter in the case $m_1 \gg m_2$) to thermal energy is $\lambda\bar{n}=0.6$ $\mu g/cm^2$, which is very close to the experimentally estimated range. The 0.038-eV cutoff is arbitrary, of course, as we have already indicated, but this is not important; setting the cutoff at 3×10^{-5} eV (i.e., $< 10^{-3}$ times thermal energy) would only double the path length and less than double the range according to Eq. (2). The extension of Eq. (2) to such energies is somewhat specious, as the thermal motion of the target atoms must be considered. But this motion results in larger scattering angles for the projectile; for example, if the thermal motion of He in He-Au collisions is neglected (as it can be, for sufficiently high energy of the Au), the maximum deflection per collision in room coordinates for the Au is only 1° (see the Appendix), but the maximum deflection will have increased to 180° by the time the Au recoil energy has decreased to approximately 0.003 eV. Thus the thermal motion in the stopping medium will make the range shorter than it would be in the absence of such motions.

According to Eq. (2) the predicted average path

lengths $\bar{n}\lambda$ down to 0.038 eV in Ne, Ar, and Xe (using thermal-energy hard-sphere cross sections for calculating λ)[30] are 0.5, 0.4, and 0.4 $\mu g/cm^2$, respectively. The ratio between range and path length can be expected to decrease from Ne to Xe because of the larger deflections. Hence, the predicted path lengths cited for He, Ne, Ar, and Xe suggest that the ranges should decrease in the order He > Ne > Ar > Xe. On the other hand, the relative kinetic energy $\frac{1}{2}\mu v^2$ [μ is the reduced mass $m_1m_2/(m_1+m_2)$] rises rapidly in order of increasing mass, probably with consequent decrease in cross section and, in turn, increase in range.

Thus, the numbers in the last column of Table I seem reasonable. Of course, the assumption of isotropic scattering in center of mass is a convenient oversimplification; a more realistic description would lead to longer predicted ranges.

We suggest the following rationalization for the shape of the A_d/A_0-vs-d plot in helium (Fig. 3 or 5):

In a series of elastic collisions, even if the scattering is not isotropic (provided only that the potential is not energy dependent), the average number of collisions necessary to reduce the energy by a given factor (say, a factor of 2) is independent of energy as in Eq. (2), i.e., is proportional to $\log(E_0/E)$. The average recoil undergoes an energy reduction of several orders of magnitude before arriving at thermal energy. Thus a doubling of E_0 from 50 to 100 eV would increase by only about 10% the number of collisions necessary to reach 0.038 eV. Moreover, the maximum deflection per collision being about 1° in helium, the path length and the range are closely related to each other. Under these circumstances it is clear that *ranges should be almost independent of energy*. This, together with the small spread in n about $\bar{n}$ (the minimum number of collisions capable of thermalizing 50-eV gold atoms in helium is about half the average number), is believed to be responsible for the shape of the range curve in helium.

ACKNOWLEDGMENTS

We wish to acknowledge the help from the operating crews of the Ford Nuclear Reactor of the University of Michigan, and from the following members of the Ford Motor Company Scientific Research Staff: Y-F. Y. Yao, H. Niki, R. G. Delosh, E. F. Gibbons, L. Terner, and the late L. R. Anders.

APPENDIX

Here we give expressions for the average cosine of the scattering angle in elastic hard-sphere collisions when the motion of the struck atom before impact can be neglected. The derivation parallels that given by Hughes (Ref. 29, pp. 25–29) for elastic scattering of neutrons.

Let the masses of projectile and struck atom be m_1 and m_2, respectively. Let the angle through which the projectile is deflected be θ in center-of-mass coordinates and φ in room coordinates. We can make a construction like that of Fig. 1-9 of Ref. 29 and find, by the law of sines,

$$\frac{\sin(\theta-\varphi)}{\sin\varphi}=\frac{m_1}{m_2}, \tag{3}$$

which gives

$$\cos\varphi=\left[1+\frac{m_2}{m_1}\cos\theta\right]\left[\left(\frac{m_2}{m_1}\right)^2+2\frac{m_2}{m_1}\cos\theta+1\right]^{-1/2}. \tag{4}$$

But the average value of $\cos\varphi$ is (see Fig. 1-9b of Ref. 29)

$$\langle\cos\varphi\rangle=\tfrac{1}{2}\int_0^{\pi}\cos\varphi\,\sin\theta\,d\theta. \tag{5}$$

Substituting (4) into (5) and integrating gives the solution, the form of which depends on the ratio between m_1 and m_2:

$$\langle\cos\varphi\rangle=\tfrac{2}{3}(m_1/m_2) \quad \text{if } m_1\leq m_2 \tag{6a}$$

$$=1-\tfrac{1}{3}(m_2/m_1)^2 \quad \text{if } m_1\geq m_2. \tag{6b}$$

Equation (1-42) of Ref. 29 is the specialization of (6a) for the case when m_2/m_1 equals A, the target mass number (neutron scattering).

From the $\langle\cos\varphi\rangle$ thus calculated, one can then calculate the average number of collisions necessary to deflect the projectile through 90°, using an expression equivalent to Eq. (1-43) of Ref. 29, that is,

$$\bar{N}=(1-\langle\cos\varphi\rangle)^{-1}. \tag{7}$$

From Eq. (4), moreover, by setting $d(\cos\varphi)/d(\cos\theta)$ equal to zero, one finds the maximum deflection per collision:

$$(\sin\varphi)_{\max}=m_2/m_1 \quad \text{when } m_1>m_2. \tag{8}$$

It is stressed that these relations hold only if the motion of the struck atoms before collision is insignificant compared to the motion of the projectile. For sufficiently low projectile energy, the thermal motion of the target atoms becomes important and the situation becomes much more complex.

[1] P. Jespersgård and J. A. Davies, Can. J. Phys. 45, 2983 (1967).

[2] J. A. Davies, J. D. McIntyre, R. L. Cushing, and M. Lounsbury, Can. J. Chem. 38, 1535 (1960).

[3] J. A. Davies, B. Domeij, and J. Uhler, Arkiv Fysik 24, 377 (1963).

[4] M. McCargo, J. A. Davies, and F. Brown, Can. J. Phys. 41, 1231 (1963).

[5] J. A. Davies, G. C. Ball, F. Brown, and B. Domeij, Can. J. Phys. 42, 1070 (1964).

[6]B. Domeij, F. Brown, J. A. Davies, and M. McCargo, Can. J. Phys. 42, 1624 (1964).
[7]J. A. Davies, Atomic Energy of Canada, Ltd., Report No. AECL-2757, 1967 (unpublished).
[8]E. V. Kornelsen, F. Brown, J. A. Davies, B. Domeij, and G. R. Piercy, Phys. Rev. 136, A849 (1964).
[9]F. Brown, G. C. Ball, D. A. Channing, L. M. Howe, J. P. S. Pringle, and J. L. Whitton, Nucl. Instr. Methods 38, 249 (1965).
[10]D. Powers, W. K. Chu, and P. D. Bourland, Phys. Rev. 165, 376 (1968); W. K. Chu, P. D. Bourland, K. H. Wang, and D. Powers, *ibid.* 175, 342 (1968).
[11]R. J. MacDonald and D. Haneman, J. Appl. Phys. 37, 3048 (1966).
[12]F. Brown and J. A. Davies, Can. J. Phys. 41, 844 (1963).
[13]L. B. Magnusson, Phys. Rev. 81, 285 (1951).
[14]S. Yosim and T. H. Davies, J. Phys. Chem. 56, 599 (1952).
[15]J. F. Emery, Oak Ridge National Laboratory Report No. ORNL-3889, 1965 (unpublished).
[16]H. Müller, Umschau Wiss. Tech. 17, 534 (1968).
[17]H. Buser and P. Graf, Angew. Chem. 66, 277 (1954).
[18]J. Pauly, Compt. Rend. 240, 2415 (1955).
[19]T. B. Novey, Atomic Energy Commission Report No. CC-1631, 1944 (unpublished).
[20]L. V. Groshev, A. M. Demidov, V. I. Pelekhov, L. L. Sokolovskii, G. A. Bartholomew, A. Doveika, K. M. Eastwood, and S. Monaro, Nucl. Data 5A, 243 (1969).
[21]C-H. Hsiung, H-C. Hsiung, and A. A. Gordus, J. Chem. Phys. 34, 535 (1961).
[22]The penetration of a moving particle into matter is best discussed in terms of the mass of material traversed (e.g., $\mu g/cm^2$)—that is, the distance multiplied by the density of the medium—rather than in terms of the distance itself (e.g., cm). In the present experiments, this convention is an obvious necessity.
[23]This can be readily seen by noting that in helium the observed recoil fraction (Fig. 3 or 5) does not decrease from the value in vacuum until there is a certain amount of helium in the gap, which implies that essentially all of the recoils have a correspondingly significant component of motion in a direction normal to the plane of the gold surface (i.e., there are few recoils emitted at low angles with the surface).
[24]J. H. Jeans, *An Introduction to the Kinetic Theory of Gases* (Cambridge U. P., Cambridge, England, 1940), pp. 53 and 54.
[25]M. Knudsen, *The Kinetic Theory of Gases: Some Modern Aspects*, 3rd ed. (Methuen, London, 1950), pp. 26–29.
[26]N. F. Ramsey, *Molecular Beams* (Oxford U. P., London, 1956), pp. 45, 46.
[27]W. Feller, *An Introduction to Probability Theory and Its Applications* (Wiley, New York, 1950), Vol. I, Sec. XIV. 8.
[28]G. Friedlander, J. W. Kennedy, and J. M. Miller, *Nuclear and Radiochemistry*, 2nd ed. (Wiley, New York, 1964), pp. 118–120.
[29]D. J. Hughes, *Pile Neutron Research* (Addison-Wesley, Cambridge, Mass., 1953), pp. 25–27.
[30]S. Dushman, in *Scientific Foundations of Vacuum Technique*, 2nd ed., edited by J. M. Lafferty (Wiley, New York, 1962), pp. 25–32.

PHYSICAL REVIEW B VOLUME 4, NUMBER 9 1 NOVEMBER 1971

Cubic-Site EPR Spectra of Eu^{2+} and Gd^{3+} in MgO Single Crystals*

M. M. Abraham, L. A. Boatner,† Y. Chen, J. L. Kolopus, and R. W. Reynolds†
Solid State Division, Oak Ridge National Laboratory, Oak Ridge, Tennessee 37830
(Received 14 June 1971)

The electron-paramagnetic-resonance spectra of Gd^{3+} and Eu^{2+} in cubic sites of MgO single crystals have been observed. Spin-Hamiltonian parameters for these ions have been determined as a function of temperature. The observed variation of the fourth-order spin-Hamiltonian parameter c vs lattice constant for the alkaline-earth oxides implies that in MgO overlap and covalency must be considered in determining the ground-state splitting of these ions.

INTRODUCTION

Although numerous electron-paramagnetic-resonance (EPR) investigations of iron-group impurities in magnesium oxide single crystals have been performed, until the recent observation[1] by EPR of Yb^{3+} in MgO, the only rare-earth resonance spectrum reported for this host was that of Er^{3+}.[2] Detailed studies of several rare-earth ions have been carried out, however, using the isomorphic (NaCl-type structure) hosts CaO, SrO, and BaO. Of these studies, the experiments[3–13] dealing with the impurity ions Eu^{2+} and Gd^{3+} ($4f^7$ configuration, $^8S_{7/2}$ ground state) are considered to be particularly significant, since they emphasize the inability of current models to account for crystal-field effects on the $^8S_{7/2}$ ground state. The cubic spectrum of Eu^{2+} in the oxides was especially interesting in that the fourth-order spin-Hamiltonian parameter was observed to vary from a positive quantity for Eu^{2+} in BaO, to approximately zero in SrO, to a negative quantity in CaO. A variation of this nature is clearly beyond the predictions of a simple crystal-field model. Additionally, the sign